Further members are possible in the preceding hierarchy of modes of classification of natural hydrosols. However, a proliferation of such modes at this time is not desirable, as it would detract attention from the only mode really worth considering in the establishment of a science of hydrologic optics, namely Mode I in either of its equivalent guises A or B. However, this ideal may not soon be reached, and accordingly the two lesser but yet extremely useful modes of classification are included in our present survey. Finally, *whenever possible and in the interests of consistency and completeness, measurements in the preceding modes should be done in the polarized light context and also as a function of time, if such is indicated by the physical (or biological) state of the medium* (cf., Sec. 13.6, 13.11).

A complete theoretical analysis and classification of the optical properties in arbitrary optical media is made in Sec. 9.6.

1.8 Colorimetric Radiative Transfer

An interesting application of radiative transfer theory can be made to the studies of the apparent colors of objects located within media that scatter and absorb radiant energy in a selective fashion. The application of the principles of radiative transfer to such studies is straightforward and requires no new concepts to be introduced into the theory beyond those we have been considering. For this purpose we need only adopt the well-known standard C.I.E. (*Commission Internationale de l'Eclairage*) color coordinate system, within which any spectral sample of radiant flux may be located and assigned a unique color, in a manner to be briefly explained below. By coupling the concepts of radiative transfer theory to the C.I.E. color coordinate system, an accurate, quantitative basis for the description of color phenomena within the atmosphere and the sea is achieved, which for the purposes of the present discussion we shall call *colorimetric radiative transfer theory*. Our goal in this section is to outline the union of the two theories and indicate the nature of its applications.

The color phenomena within the domain of colorimetric radiative transfer theory are manifold: a precise description and prediction is possible of the blue of the sky and of the reds and golds of sunsets; of the onset and growth of the blue and purple hazes between distant mountains and a receding observer; the odd yellowing of mercury vapor street lamps with distance in strange blue fogs [177]; the conventional but ever pleasant sight of a reddish-orange rising moon; the yellowing and reddening of extremely shiny surfaces such as corrugated aluminum roofs and sidings seen through long paths of sight in the atmosphere; the sickening brown smear of smog smothering a city. In the underwater domain, the colorimetric radiative transfer phenomena are overpowered and dominated by the highly selective absorption of reds and violets (and their neighboring colors), resulting in a powerful filtering of all sky light into a blue-green residue of greater or lesser luminance that pervades almost all submarine scenes.

Brightly-colored submerged tropical scenes of plants and animals with their reds, yellows and deep blues quickly transform with distance into shades of brighter or dimmer greens and blues with reds and purples washed to pink and then attenuated away. Such scenes are now easily witnessed firsthand with modern scuba devices. However, only one or two generations ago, such sights were a rare delight.

In his 1927 Haiti expedition, Beebe [12] noted that:

> "Toward the end of the dive I sat on white sand [in his diving helmet rig] and watched the surface above me. The sea breeze had sprung up and it was fairly rough. The view from beneath was of green, wrinkled, translucent ceiling cloth, never still for a moment, crinkling and uncrinkling, waving and flapping as in a breeze, or rather cross breezes. It was decidely green in comparison with the ever more blue distance--turquoise green in the sunlight, changing toward greenish glaucous in shadow. As to the distance, I can never get away from the idea of the most diluted, ethereal ultramarine, and yet my mind knows that a dozen other colors are somehow in it."

All of these phenomena can be quantitatively and quite accurately described by means of such simple models for radiance and irradiance as developed in Sec. 1.3, which need only use information on optical properties obtainable by Mode III classification procedures of optical media (cf., Sec. 1.7).

The Quantitative Description of Color

It is a relatively easy matter to understand the C.I.E. color coordinate system if we recall some similar conventions we have adopted in our everyday tasks of locating objects in space. Part (a) of Fig. 1.75 exhibits an object in space (designated by "A") which can be located by means of its three coordinates in an xyz cartesian frame of reference. There is nothing unique about this frame as far as being adequate to locate A in space. The alternate frame depicted in (b) of Fig. 1.75 will do just as well. In each diagram, object A is located at the same spot. That spot, fixed relative to the first frame, is designated by a vector **u** which is specified by giving its coordinates (x,y,z). These coordinates are found by dropping perpendiculars from **u** to each of the three axes, in short, by finding the dot products:

$$\mathbf{u} \cdot \mathbf{i} \tag{1}$$

$$\mathbf{u} \cdot \mathbf{j} \tag{2}$$

$$\mathbf{u} \cdot \mathbf{k} \tag{3}$$

of the vector **u** with the mutually orthogonal unit vectors **i**, **j**, **k** along the x, y, z axes respectively. This is called *analyzing* **u** relative to the x, y, z frame. The next step is to *synthesize* **u** (i.e., get it back) by means of the equation:

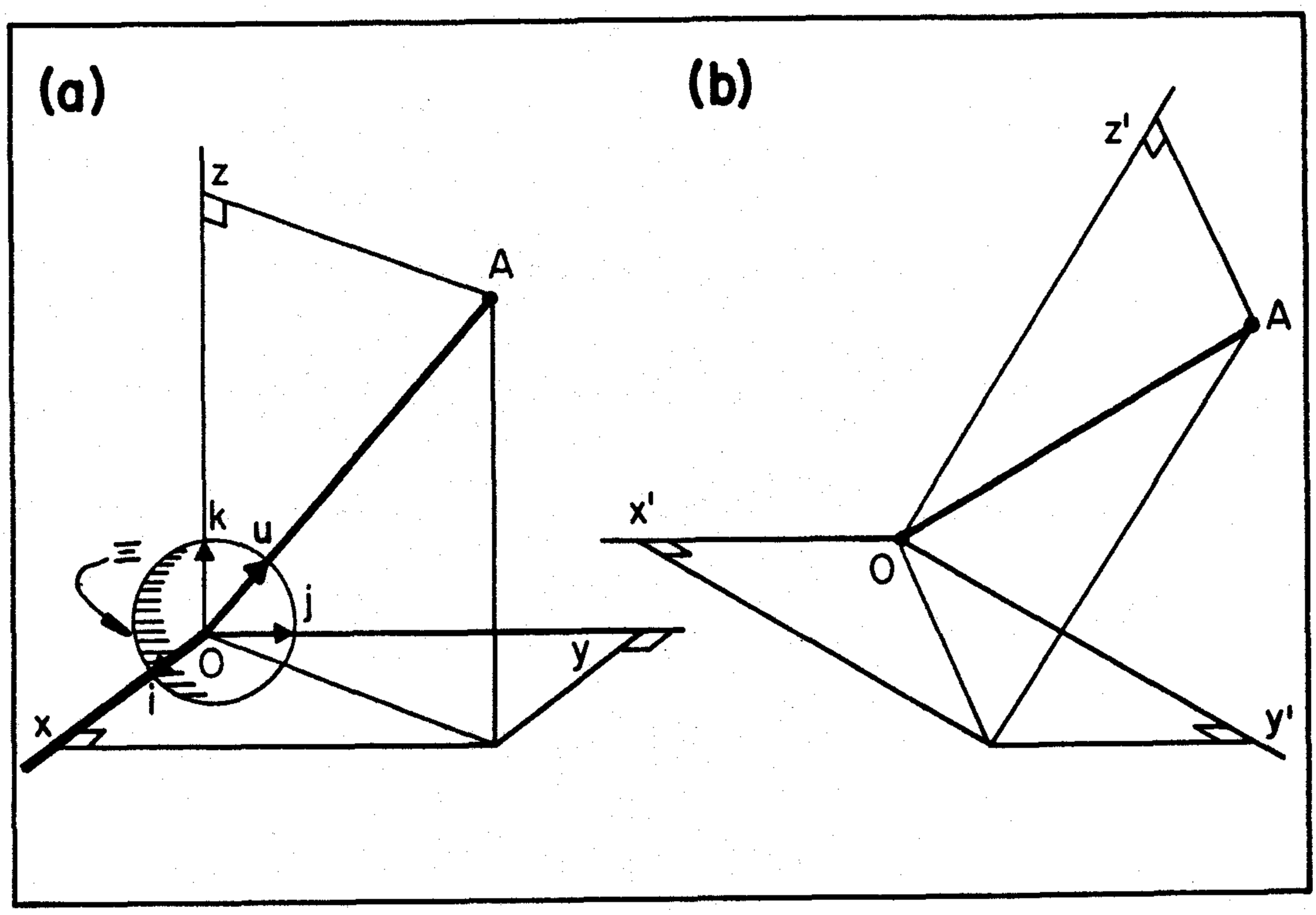

FIG. 1.75 For illustrating the analogy between coordinate systems in the real three dimensional world and the C.I.E. tristimulus color coordinate system.

$$\mathbf{u} = (\mathbf{u}\cdot\mathbf{i})\mathbf{i} + (\mathbf{u}\cdot\mathbf{j})\mathbf{j} + (\mathbf{u}\cdot\mathbf{k})\mathbf{k} \qquad (4)$$

Now, we can perform such an analysis and synthesis not only on a simple location vector such as **u**, but also on any radiant flux function P defined on the electromagnetic spectrum Λ (the set of all wavelengths from $\lambda = 0$ to $\lambda = \infty$). Instead of the **i**, **j**, **k** unit vectors, we now use the (dimensionless) *tristimulus functions* $\bar{x}$, $\bar{y}$, $\bar{z}$ on Λ adopted by the C.I.E.. A plot of each of these is given, to scale, in Fig. 1.76. If we form samples of radiant flux with just the power spectra given by the forms of these three functions, then the visual sensation of the $\bar{x}$ sample would be red, that of $\bar{y}$ would be green, and that of $\bar{z}$, blue.

To analyze a given radiant flux sample P (watts/mμ) into its red, green and blue components, we write:

$$\text{"}P\cdot\bar{x}\text{"} \quad \text{for} \quad 680\int_0^\infty P(\lambda)\,\bar{x}(\lambda)\,d\lambda \quad \text{(lumens)} \qquad (5)$$

$$\text{"}P\cdot\bar{y}\text{"} \quad \text{for} \quad 680\int_0^\infty P(\lambda)\,\bar{y}(\lambda)\,d\lambda \quad \text{(lumens)} \qquad (6)$$

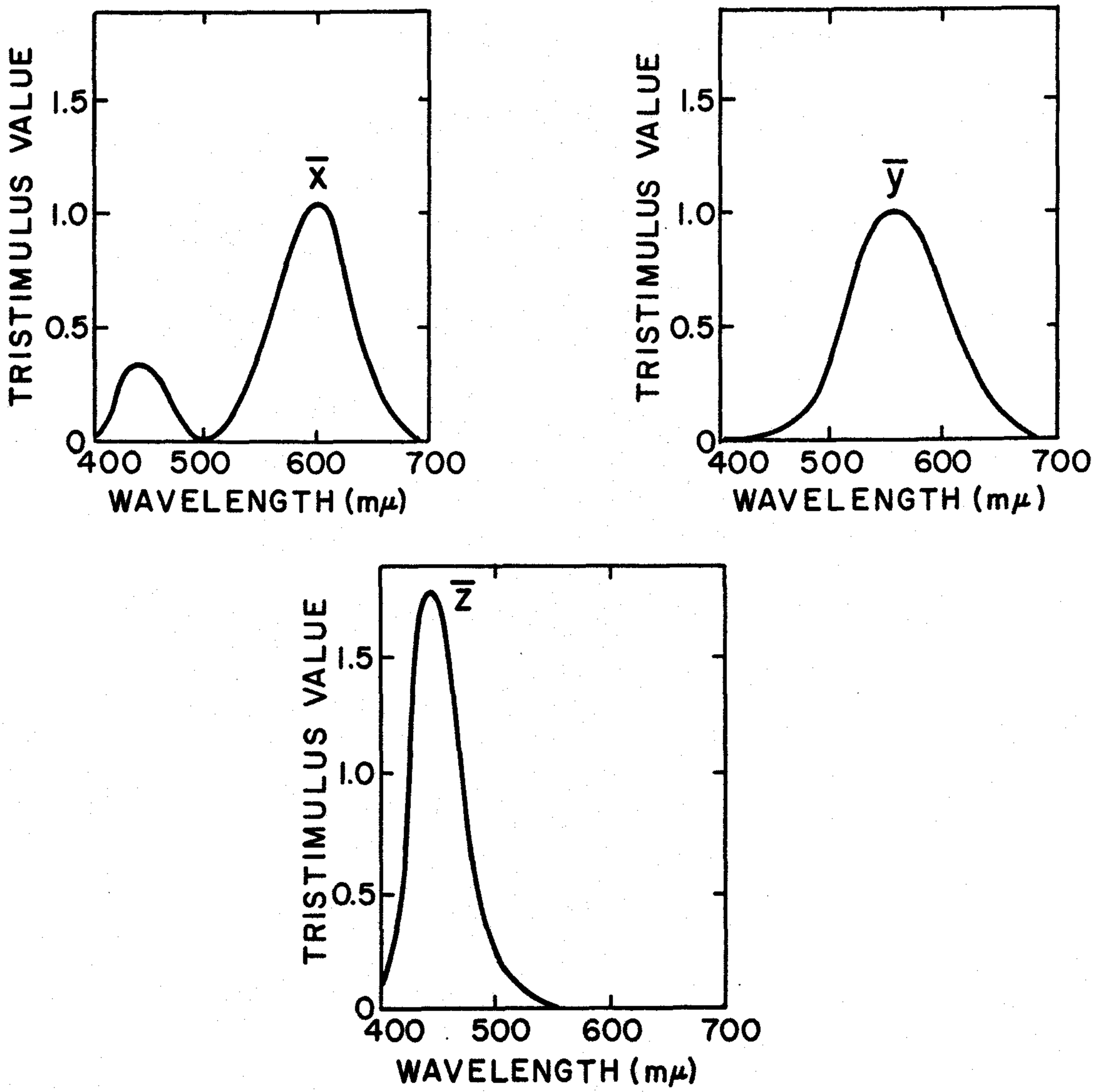

FIG. 1.76 The tristimulus functions. The $\bar{y}$ curve is the photopic luminosity function of Fig. 1.10.

$$\text{"P}\cdot\bar{z}\text{"} \quad \text{for} \quad 680\int_0^\infty P(\lambda)\ \bar{z}(\lambda)\ d\lambda \qquad \text{(lumens)} \qquad (7)$$

which are closely analogous to the simple vector operations (1), (2), (3). The number 680 has dimensions of lumens/watt, and serves as a connection with photometry--(cf., Sec. 2.12). To point up this similarity to the vector operations we have written "$P\cdot\bar{x}$", "$P\cdot\bar{y}$", and "$P\cdot\bar{z}$" for (5), (6), (7), respectively. Then analogously to (4) we can synthesize these components. We do this and write:

$$\text{"}\subset[P]\text{"} \quad \text{for} \quad (P\cdot\bar{x})\bar{x} + (P\cdot\bar{y})\bar{y} + (P\cdot\bar{z})\bar{z} \qquad (8)$$

We call $C[P]$ the *color* or *chromaticity* of P. $C[P]$ is a function defined on Λ and it is designed to give a very close visual color match to the original function P. The point to observe here is that whereas P could be of quite an arbitrary structure over Λ, its color $C[P]$ is the linear superposition of three suitably weighted amounts of standard red, green, and blue radiant flux samples. The weighting numbers $P\cdot\bar{x}$, $P\cdot\bar{y}$, $P\cdot\bar{z}$ are the *color components* of P, and the ordered triple of numbers $(P\cdot\bar{x}, P\cdot\bar{y}, P\cdot\bar{z})$ is the *color vector* associated with P. In this way we have set up a one-to-one transformation of given radiant flux samples P into their associated colors $C[P]$, each with three well defined color components* $P\cdot\bar{x}$, $P\cdot\bar{y}$, $P\cdot\bar{z}$. For brevity let us write (in accordance with C.I.E. notation):

$$\text{"X"} \quad \text{for} \quad P\cdot\bar{x} \tag{9}$$

$$\text{"Y"} \quad \text{for} \quad P\cdot\bar{y} \tag{10}$$

$$\text{"Z"} \quad \text{for} \quad P\cdot\bar{z} \tag{11}$$

We observe in passing that the component $P\cdot\bar{y}$ of a sample P of radiant flux is simply its photometric counterpart. Thus, for radiance N, $N\cdot\bar{y}$ is the associated luminance B; for irradiance H, $H\cdot\bar{y}$ is the associated illuminance E; and so on (cf., Sec. 1.1). Tables of $\bar{x}$, $\bar{y}$, $\bar{z}$ along with further descriptions of colorimetry may be found in [50].

We may summarize the analogy between simple location vectors and chromaticity vectors by means of the parallel listings below in Table 1.

TABLE 1

A vector analogy for chromaticity concepts

Location Vectors	Chromaticity Vectors
(1) Original vector **u**	(1) Original radiant flux function P
(2) **i,j,k** unit vectors	(2) $\bar{x},\bar{y},\bar{z}$ tristimulus functions
(3) Components of **u** with respect to **i,j,k** : $\mathbf{u}\cdot\mathbf{i} = \alpha$ $\mathbf{u}\cdot\mathbf{j} = \beta$ $\mathbf{u}\cdot\mathbf{k} = \gamma$	(3) Color components of P with respect to $\bar{x},\bar{y},\bar{z}$: $P\cdot\bar{x} = X$ $P\cdot\bar{y} = Y$ $P\cdot\bar{z} = Z$
(4) The representation of **u**: $\mathbf{u} = \alpha\mathbf{i} + \beta\mathbf{j} + \gamma\mathbf{k}$	(4) The representation of P: $C[P] = X\bar{x} + Y\bar{y} + Z\bar{z}$

*The mathematical reader will see that this vector terminology is completely appropriate, for what we can postulate initially is the vector space $\mathscr{P}$ of all Riemann integrable functions P on Λ. The mapping C is therefore a non-identity linear transformation of $\mathscr{P}$ into itself. It turns out that C is one-to-one and not onto, but its range is sufficiently large to encompass most colors seen by the human eye.

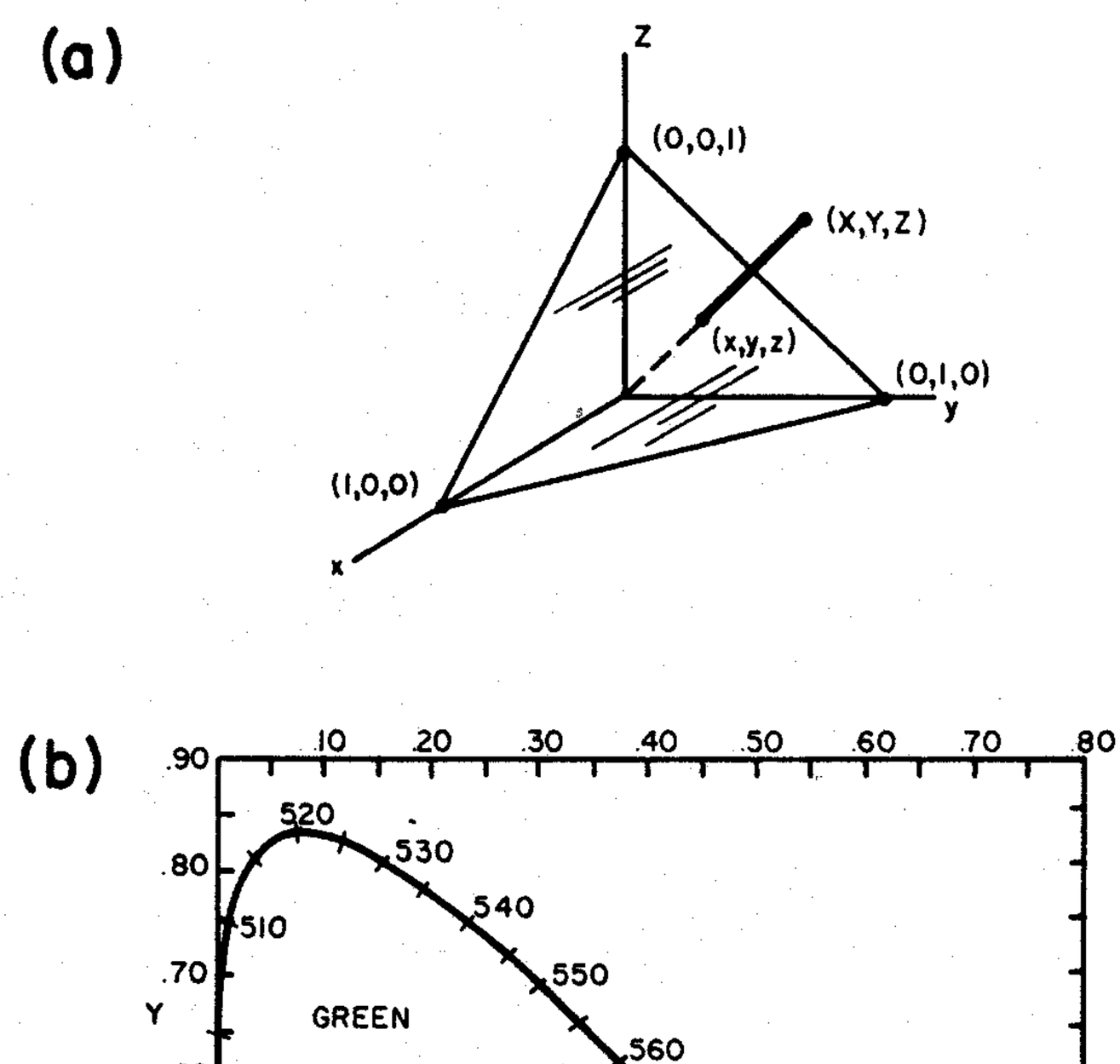

FIG. 1.77 Chromaticity plane (part (a)) and chromaticity diagram (part (b)). Point E is the white-light point.

In the usual location vector theory, a special place is reserved for vectors of unit length, namely the unit sphere Ξ shown in (a) of Fig. 1.75. Analogous to the unit sphere is the *chromaticity plane* shown in (a) of Fig. 1.77. This plane has the property that for all points p (= (x,y,z)) on it we have x+y+z = 1. If (X,Y,Z) is a chromaticity vector, then the vector

$$\frac{1}{(X+Y+Z)} \cdot (X,Y,Z) = \left(\frac{X}{X+Y+Z}, \frac{Y}{X+Y+Z}, \frac{Z}{X+Y+Z}\right)$$

lies on the chromaticity plane. Observe that only the part of the chromaticity plane that lies in the first octant (shown in (a) of Fig. 1.77) is needed in colorimetry. For, since P and the functions $\bar{x}$, $\bar{y}$, $\bar{z}$ are never negative, all chromaticity vectors accordingly lie in the first octant. Observe further

that one need only use two numbers to locate a point on the chromaticity plane. These numbers are conventionally chosen to be the x and y components, where we write

$$\text{"x"} \quad \text{for} \quad \frac{X}{X+Y+Z} \tag{12}$$

$$\text{"y"} \quad \text{for} \quad \frac{Y}{X+Y+Z} \tag{13}$$

$$\text{"z"} \quad \text{for} \quad \frac{Z}{X+Y+Z} \tag{14}$$

The x,y,z are the *chromaticity components* (or *coordinates*) of P. By projecting all chromaticity vectors (X,Y,Z) down onto the chromaticity plane, as shown in Fig. 1.76, we are in effect normalizing the associated luminances of the radiant flux function P. Once the chromaticity plane is defined we can excise it from its spatial context, or simply work with a plane diagram copy of the chromaticity plane, as in (b) of Fig. 1.77. The x and y chromaticity coordinates are displayed in a way once again reminiscent of the usual location vector conventions.

Once the setting in (b) of Fig. 1.77 is achieved, we can locate within it all manners of points which represent the conventional colors of familiar everyday objects and scenes. For example, suppose that we begin with a sample P of radiant flux which has a constant value P_o for all λ. From (5)-(7) this gives:

$$X = 680\ P_o \int_0^\infty \bar{x}(\lambda)\ d\lambda \tag{15}$$

$$Y = 680\ P_o \int_0^\infty \bar{y}(\lambda)\ d\lambda \tag{16}$$

$$Z = 680\ P_o \int_0^\infty \bar{z}(\lambda)\ d\lambda \tag{17}$$

Now the $\bar{x}$, $\bar{y}$, and $\bar{z}$ functions are so designed that their integrals over $\Lambda = [0,\infty]$ have essentially a single common value, namely 21.37. Hence the associated chromaticity components for this P are

$$x = 1/3$$

$$y = 1/3$$

$$z = 1/3$$

Such a flux sample has the appearance of a pure white color and is analogous to pure noise in acoustics. In fact, in the

theory of stochastic processes, if the spectrum of a given function is of constant value, it is said that the function represents *white noise* (all the analogies we are touching here and there in the present exposition are quite deep and far more than superficial in appearance).

The point (x,y) = (1/3,1/3) in the chromaticity plane corresponding to *white light* is denoted by "E", in (b) of Fig. 1.77 and is the central base of operations in the practical task of specifying colors. If we go on to obtain the chromaticity coordinates of all the pure monochromatic colors of the spectrum Λ (their sample functions P are Dirac delta functions), we sweep out a horseshoe shaped locus in the plane of (b) of Fig. 1.77, starting approximately at the point x = .74, y = .26 (red), and sweeping around to the point x = .07, y = .84 (green), and ending up at x = .17, y = .01 (violet). This curve is called the *spectrum locus*. We can close the locus by drawing the straight line from the violet to the red point. The closed plane region so formed is the *chromaticity diagram*. The colors associated with the points of the spectrum locus are the purest colors attainable in the present system. Suppose that a given sample of radiant flux has chromaticity coordinates (x,y) which land it at point Q on the chromaticity diagram. Draw a straight line from E through Q to intersect the spectrum locus at W. The wavelength λ associated with W is called the *dominant wavelength* or *color* of Q, and the fraction p = EQ/EW (where "EQ", "EW" denote the lengths of the respective straight line segments) is called the *purity* of the color of Q. If a point such as Q' is considered, we extend Q'E back to W', and the associated purity is by definition EQ'/EW'. *In this way, we finally achieve the first part of our goal for the present exposition, namely, the explanation of how a given sample* P *of radiant flux defined on the spectrum* Λ *can be assigned two numbers: its dominant wavelength* λ *and the purity* p *of the dominant wavelength of* P.

These two numbers act very much like the polar coordinates of points in the chromaticity diagram, with the point E as the pole. The purity is often given as a percentage rather than a fraction. Hence the pair (x,y) of chromaticity coordinates have their polar equivalents (λ,p). We shall use the term "chromaticity coordinates" interchangeably for these equivalent representations.

An Example of Experimentally Determined Chromaticity Coordinates

We shall now cite some examples of the preceding concepts. These examples are drawn from various colorimetric studies of natural hydrosols. Fig. 1.78 depicts the spectral dependence of the apparent radiance of submerged sandy shoals and reefs as studied in 1944 by Duntley through a glass-bottomed boat surveying parts of the east coast of Florida (near Dania). The same submarine area surveyed from an altitude of 4300 feet (1300 meters) is depicted in Fig. 1.79. If $N(\lambda)$ is the apparent radiance of a particular point of the underwater

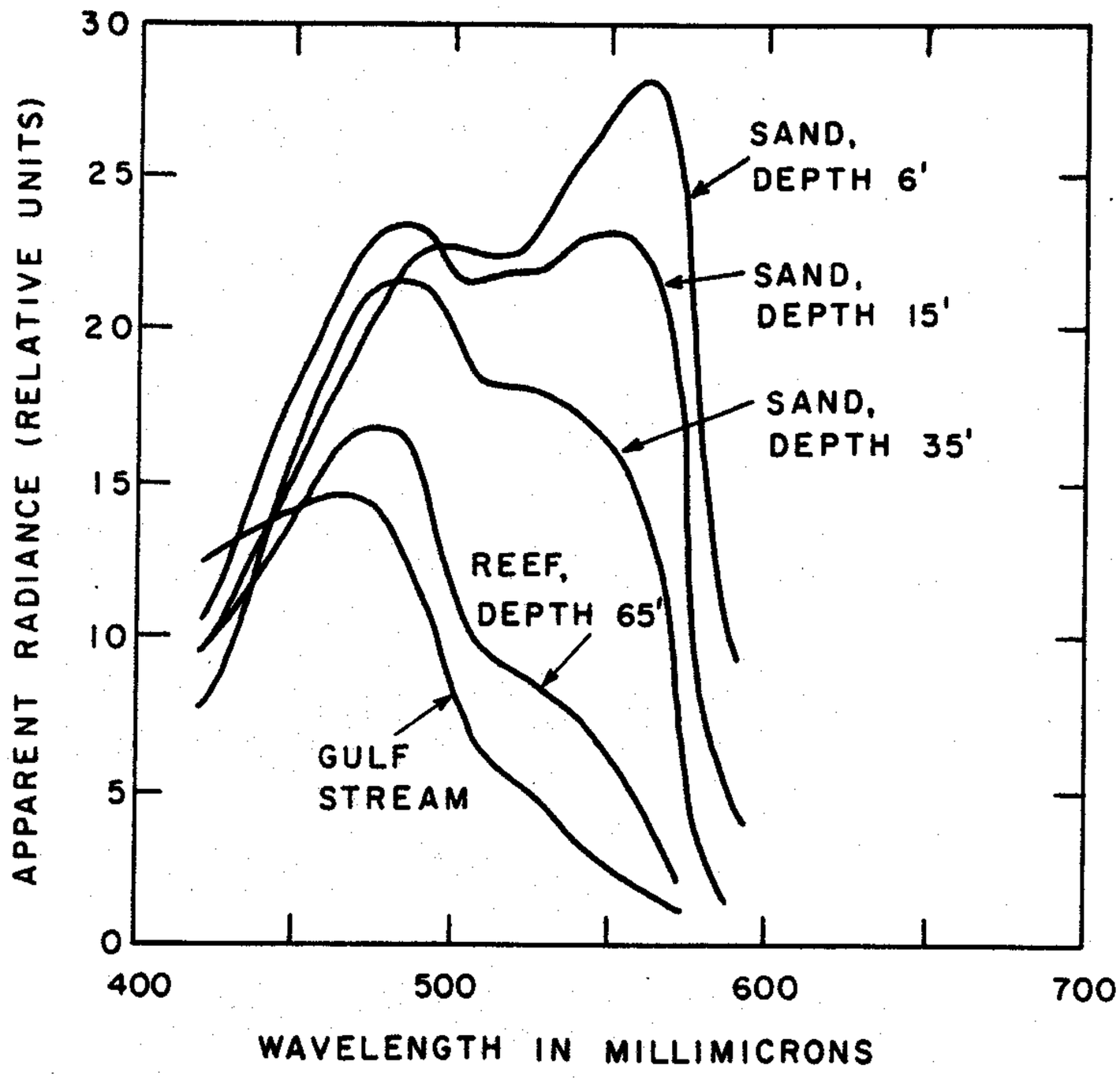

FIG. 1.78 Spectroradiometric curves of sandy bottom of shoals near Dania, Florida, by Duntley, March 1944. (Fig. 1 from [78], by permission)

scene for a given λ, as plotted on Fig. 1.78, then the color components x, y, z of $N(\lambda)$, $0 \leqq \lambda \leqq \infty$, are obtained by using these plotted radiance values in (5)-(7) and (12)-(14) with $N(\lambda)$ replacing $P(\lambda)$. Seventy-six chromaticity coordinates x, y, were computed according to (12), (13) for each of the five curves in Fig. 1.78, and their locations are shown along the upper curve on the chromaticity diagram of Fig. 1.80. The corresponding

Errata

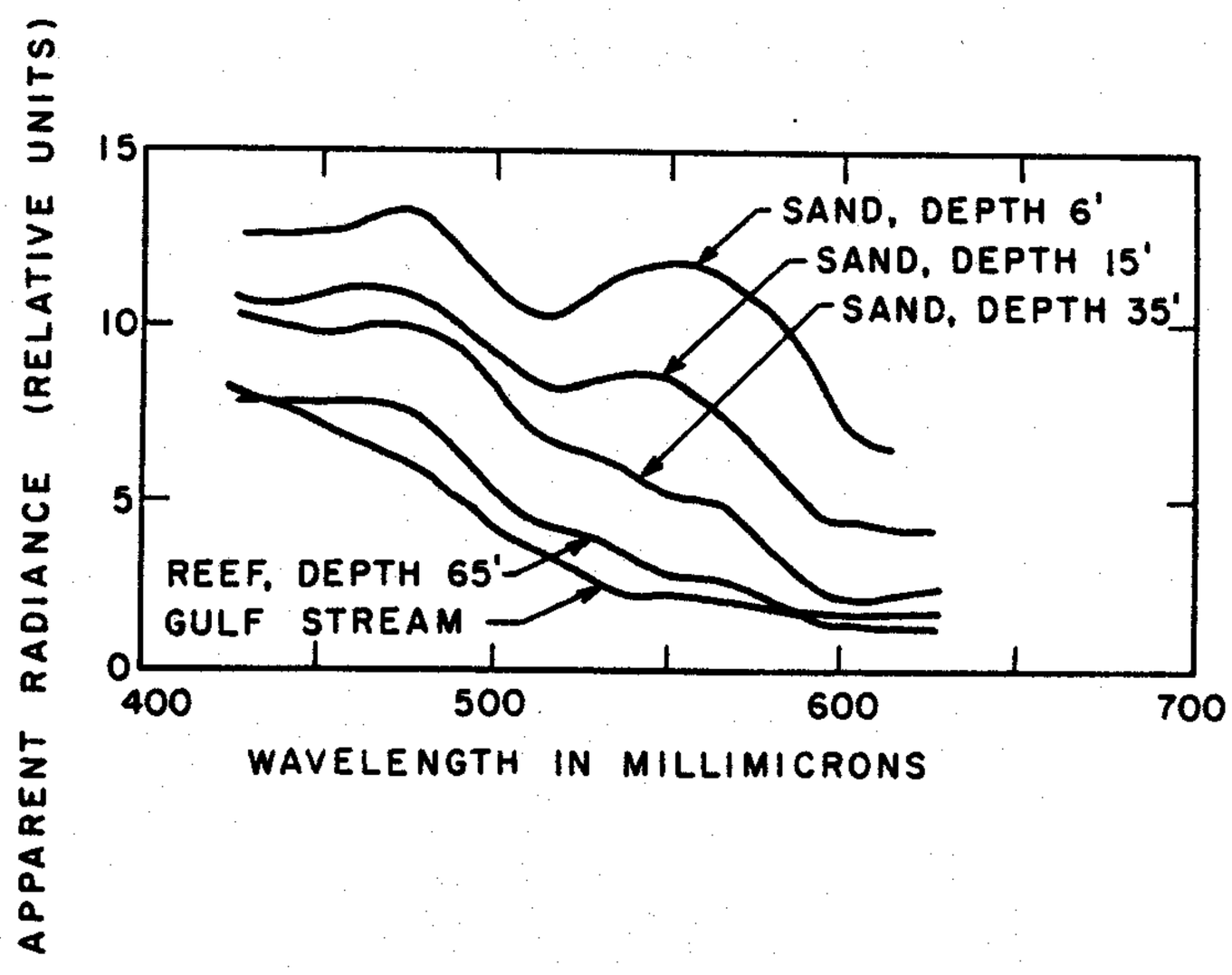

FIG. 1.79 Same scene as Fig. 1.78, viewed from an altitude of 4300 feet. (Fig. 2 from [78], by permission)

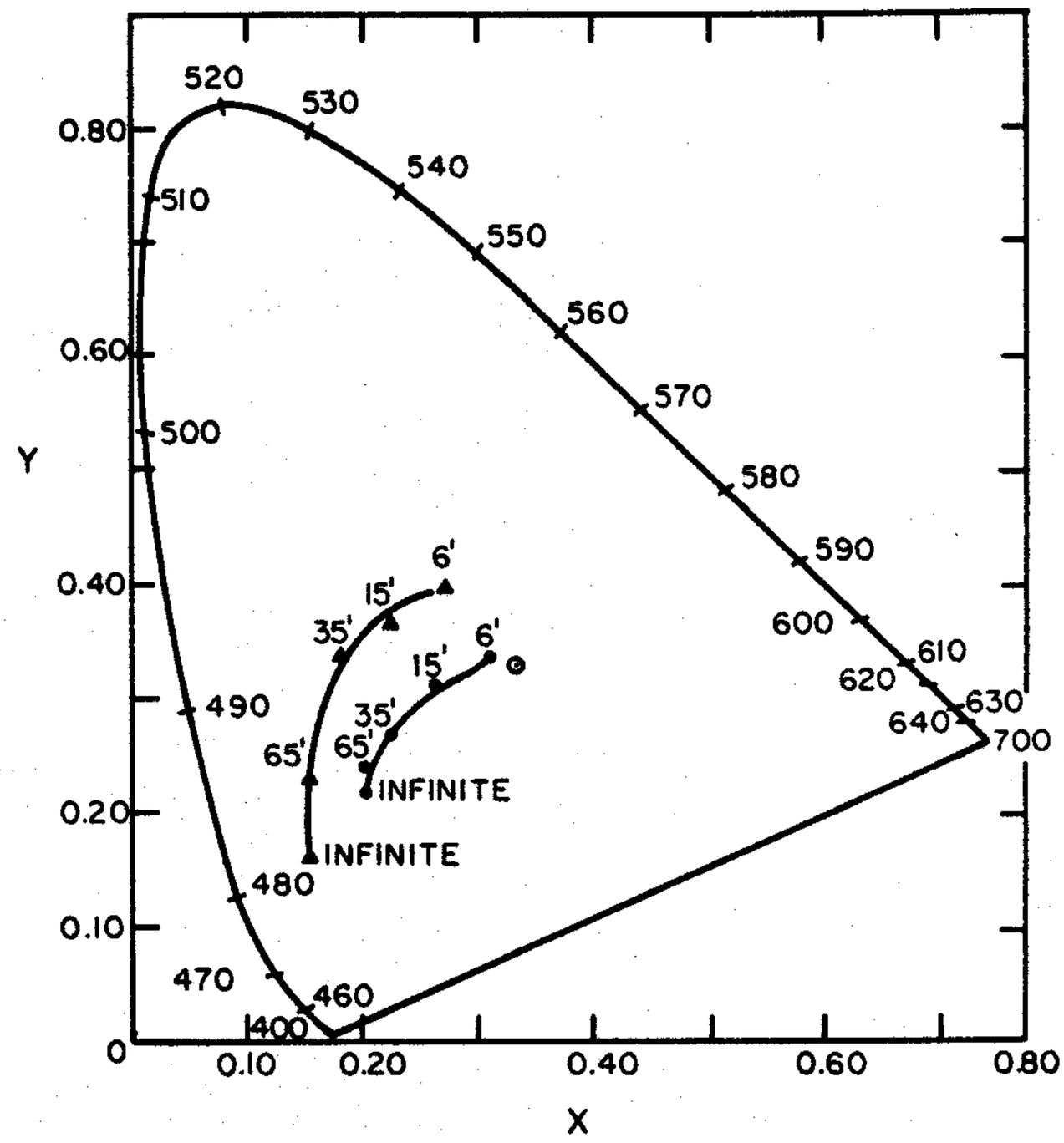

FIG. 1.80 Chromaticity diagram associated with the curves of Figs. 1.78, 1.79. The five curves of Fig. 1.78 yield the five points of the upper curve in the chromaticity diagram. The five curves of Fig. 1.79 yield the five points of the lower curve in the diagram. (Fig. 3 from [78], by permission)

locus of the chromaticity coordinates for the aerial view of the shoals is given by the lower curve in Fig. 1.80. This example is taken from the review article [78] by Duntley. Further examples may be found in [126], and [302].

We now turn to the second part of our goal in this section, the theory of colorimetric radiative transfer.

On the Use of Simple Models for Theoretical Predictions of Chromaticity Coordinates

A relatively unexplored area of application of the simple models for radiance and irradiance developed in Sec. 1.3 is colorimetric radiative transfer theory. We shall consider the essential steps that may be taken in this direction of application. Starting quite generally with the apparent radiance form of the equation of transfer (12) of Sec. 1.3, let us take the wavelength λ out of wraps and write the equation with λ explicitly shown, as follows:

$$N_r(z,\theta,\lambda) = N_o(z_o,\theta,\lambda)e^{-\alpha(\lambda)r} + \int_0^r N_*(z',\theta,\lambda)e^{-\alpha(\lambda)(r-r')}dr' \quad (18)$$

By specifying $N_o(z_o,\theta,\lambda)$, $\alpha(\lambda)$, and $N_*(z',\theta,\lambda)$ we are able in principle to compute $N_r(z,\theta,\lambda)$ for every z, θ, r, and λ over given paths and for a preselected set of λ values in Λ. Then by (5)-(7), we can compute:

$$X_r(z,\theta) = 680\int_0^\infty N_r(z,\theta,\lambda)\ \bar{x}(\lambda)\ d\lambda \tag{19}$$

$$Y_r(z,\theta) = 680\int_0^\infty N_r(z,\theta,\lambda)\ \bar{y}(\lambda)\ d\lambda \quad (=B_r(z,\theta)) \tag{20}$$

$$Z_r(z,\theta) = 680\int_0^\infty N_r(z,\theta,\lambda)\ \bar{z}(\lambda)\ d\lambda \tag{21}$$

From these color components of $N_r(z,\theta,\lambda)$, using (12), (13), we can find the two chromaticity coordinates:

$$x_r(z,\theta) = \frac{X_r(z,\theta)}{X_r(z,\theta) + Y_r(z,\theta) + Z_r(z,\theta)} \tag{22}$$

$$y_r(z,\theta) = \frac{Y_r(z,\theta)}{X_r(z,\theta) + Y_r(z,\theta) + Z_r(z,\theta)} \tag{23}$$

and from these, as explained above, we derive the dominant wavelength λ and the purity p of this wavelength. Such a pair (λ,p) is a function of z, θ, and r, and we thus may write the pair as: $(\lambda_r(z,\theta),\ p_r(z,\theta)\ )$.

The simple model for apparent radiance (14) of Sec. 1.3 should be a rich source of colorimetric predictions for the light fields in natural hydrosols. Thus we can now write the equation as:

$$N_r(z,\theta,\lambda) = N_o(z_o,\theta,\lambda)e^{-\alpha(\lambda)r} + \frac{N_*(z,\theta,\lambda)}{(\alpha(\lambda)+K(\lambda)\cos\theta)}\left[1-e^{-(\alpha(\lambda)+K(\lambda)\cos\theta)r}\right] \tag{24}$$

where

$$N_*(z,\theta,\lambda) = N_*(0,\theta,\lambda)e^{-K(\lambda)z}$$

By setting $\theta = 0$, $\pi/2$ and π in (24), for example, we can predict the spectral apparent radiance of the hydrosol in these directions at depth z and via (22), (23), assign dominant wavelengths to these directions and depths, and purities to these wavelengths. To use (24) one need only specify $\alpha(\lambda)$, $K(\lambda)$ and $N_*(0,\theta,\lambda)$ along with $N_o(z_o,\theta,\lambda)$. The equation will then automatically take care of and predict the effects of the radiative transfer processes on the apparent radiances $N_r(z,\theta,\lambda)$.

The quantitative study of the colors of distant objects was apparently first systematically done by Middleton [177] in the meteorologic optics setting. He used a special case of (24) in which $\theta = \pi/2$, and computed the change in color of various objects as a function of r. His computation may serve as a model for the more extensive computations that can be made using (24) with a general value of θ.

In a completely similar way we may use the two-flow model for spectral irradiance $H(z,\pm,\lambda)$ described in (6), (7) of Sec. 1.3, and particularly in (8)-(10) of Sec. 1.4, to predict the chromaticity coordinates of the upward and downward irradiances as a function of optical depth in a given medium. The λ-dependence of $H(z,\pm,\lambda)$ enters this theory via the γ parameter and also the initial irradiances $H(0,\pm,\lambda)$ (or any equivalent pair of irradiances, as suggested by (43), (44) of Sec. 1.4).

It should be observed that in the employment of the simple model for radiance and the two-flow model for irradiance, we require only information on the Mode III level of classification of natural hydrosols (cf., Sec. 1.7).

Our purpose in this brief excursion into the world of submarine color has been to lay the foundations for a scientific description of the myriads of colors and their many hues as seen beneath the surface of seas and lakes illuminated by natural light. The simple theory evolved above and culminating in (22) and (23) goes a long way toward a quantification of the otherwise inexpressible color sensations experienced by all who explore and study underwater environs. Even such skilled expositors of natural phenomena as Minnaert [182] or William Beebe were hard pressed in their explorations of the atmosphere and the sea to describe adequately what they saw. In his studies of the coral reefs of Haiti in 1927, Beebe, in particular, observed that [12]:

> "Someday, when I can carry a color book in my helmet, I will be able to enumerate an exact color code of distance. Even in our colder, thinner atmosphere the green of mountain slopes softens to purple a long way off, but on the bottom of the sea, still greater changes take place within a few feet or yards. I have walked backward and seen a feathery-crowned sea-worm of dragon's blood alter, in my vision, within a few seconds and steps, to the palest of coral pink; while a sea-weed, deep olive-green when within reach, comes gently to the eye, when five yards away, as faintest glaucus."

The relatively precise expression of these transformations of colors with distance in scattering-absorbing media is now within our grasp. But the placing of a coordinate grid over our visual impressions can go only so far--something of our impressions of the real world will always slip through such a coarse net. This was sensed by Beebe; and for us, now in possession of the relatively powerful tools forged above, we are inclined to agree when he goes on to reflect that [12]:

> "An artist of great skill and patience can approximate the oxydized royal purple of a gorgonia, even

the pink and ivory sunset of a conch shell--but the vanishing point of distance beneath the water, where the coral reef ends and the mysteries of the unknown deeps begin--the illusion, too subtle for color, of submarine visual infinity--this is not to be whelmed by man-made brushes nor imprisoned on any terrestrial dimension."

<< Table of Contents << Title Page >> Next Page >>

1.9 Applications of Hydrologic Optics to Underwater Visibility Problems

In this section we shall apply the simple model for radiance (14) of Sec. 1.3 to the problem of predicting the visibility of underwater objects illuminated by natural light fields and as seen by underwater swimmers. In order to achieve this goal we must take into account not only the geometrical structure of the light field at each depth z, and its general exponential decrease with depth, but also the inherent properties of the eyes of the underwater swimmer and their mode of adaptation to the light levels in the underwater environs. These rather delicate features of the problem must be blended with great care in order to achieve a synthesis which is at once readily applicable under rugged field conditions, and yet accurate enough to make useful and dependable predictions.

Such a synthesis has recently been achieved by Duntley and it is on his results reported in [75] that the present section is based. Except for minor changes of the text of [75], in order to insure continuity within the framework of the present work, the exposition of the use of the nomographs is essentially that given in [75]. Successful experimental field tests of the theory underlying the simple model are recorded in [83]. (See Figs. 1.51, 1.52.)

We observe that the optical properties required for the application of the nomographs in this section are the volume attenuation coefficient α and the diffuse attenuation coefficient K, so that we require only a Mode III classification of optical media, as defined in Sec. 1.7, in order to implement the theoretical results summarized below. These optical properties may be measured simultaneously by means of a water clarity meter designed and developed at the Visibility Laboratory of the Scripps Institution of Oceanography [7] and which has been in use now for several years by the U.S. Oceanographic Office.

Introduction to the Nomographs

The limiting range at which a swimmer can sight any specified underwater object can be calculated from α and K if sufficient information is available concerning the nature of the object, its lighting, its background, and the visual characteristics of the observer. Consider, for example, the two underwater photographs shown in Fig. 1.81. In part (a) of the figure the camera is looking steeply downward through twenty